

ENSO Impact on the Declining CO₂ Sink Rate**Roy W Spencer****Earth System Science Center, University of Alabama in Huntsville, USA****Corresponding Author**

Roy W Spencer, Earth System Science Center, University of Alabama in Huntsville, USA.

Submitted: 2023, June 30; **Accepted:** 2023, July 19; **Published:** 2023, July 25**Citation:** Spencer, R. W. (2023). ENSO Impact on the Declining CO₂ Sink Rate. *J Mari Scie Res Ocean*, 6(4), 163-170.**Abstract**

The ocean and land processes which determine the rate of uptake of anthropogenic carbon dioxide emissions are many and complex. Simplified models of the net effect of all these processes can assist in the development of more detailed models. A simple time-dependent atmospheric CO₂ budget model is shown to closely match yearly Mauna Loa CO₂ concentrations during 1959-2021. The model assumes an anthropogenic CO₂ source, and a constant yearly CO₂ sink rate proportional to the excess of CO₂ over a baseline equilibrium value determined by the Mauna Loa data. The yearly CO₂ sink rate is found to be 2.02% of the atmospheric excess above 293.6 ppm, with a downward trend in the sink rate during 1959-2021 that disappears when El Niño – Southern Oscillation (ENSO) activity is empirically accounted for. Significant model departures from observations occurred for three years after the 1991 eruption of Mt. Pinatubo. Assuming no change in the sink rate, the latest Energy Information Administration CO₂ global emissions projections to 2050, and extrapolated to 2100, lead to model-projected CO₂ concentrations well below the highest Representative Concentration Pathways scenario RCP8.5.

Key Points

1. A CO₂ budget model forced with human emissions and ENSO activity closely matches yearly Mauna Loa, HI CO₂ measurements during 1959-2021.
2. Contrary to previously published results there is no decreasing trend in the CO₂ sink rate of 2.02% of the yearly excess over 293.6 ppm.
3. Projections of CO₂ emissions results in model CO₂ levels well below the IPCC RCP8.5 scenario through 2100, reducing climate impacts.

Plain Language Summary

While the biological and physical processes which remove excess CO₂ from the atmosphere are numerous and complex, a simple time-dependent CO₂ budget model is shown to closely match yearly CO₂ measurements at Mauna Loa, Hawaii during 1959-2021. After correction for El Niño and La Niña influences on the data, and using yearly estimates of global anthropogenic CO₂ emissions, the Mauna Loa data suggest the Earth system has been removing excess CO₂ at a constant yearly rate of 2.02% of the atmospheric excess above an effective equilibrium level of 293.6 ppm, which is somewhat above the pre-industrial level of 280 ppm. Contrary to previously published calculations and carbon cycle model projections, these results suggest the CO₂ removal rate has not yet decreased. The removal rate was briefly doubled after the 1991 eruption of Mt. Pinatubo due to increased photosynthesis. Using recent estimates of future increases in global CO₂ emissions, and assuming no future decrease in the sink rate, the amount of CO₂ in the atmosphere by 2050 and 2100 is estimated to be in the mid-range of future emissions scenarios currently being used by climate models, but well below the most extreme scenario.

Keywords: Biogeochemical Cycles, Carbon Dioxide, Climate Variability, Climate Change.**1. Introduction**

The Earth system processes which govern the rate of removal of excess atmospheric CO₂ resulting from anthropogenic fossil fuel burning are numerous and complex [1,2]. Complicating the analysis are natural fluctuations in the climate system such as El Niño and

La Niña activity, as well as major volcanic eruptions [3,4]. There is some evidence that the rate of removal of excess CO₂ from the atmosphere has been declining over the last half-century, a result which would lead to higher atmospheric CO₂ concentrations in the future and presumably enhanced levels of climate change [4-6].

The CO₂ sink rate is critical to projections of climate change. Future CO₂ concentration estimates such as the IPCC Representative Concentration Pathways (RCP) scenarios provide various projections of global climate change and involve differing assumptions about (1) global economic activity and the carbon-intensiveness of those activities, and (2) global carbon cycle changes which remove excess CO₂ from the atmosphere [7].

Here, the latter process is inferred in the most basic of terms as a yearly, global net value from the differences between yearly global anthropogenic CO₂ emissions and measurements of the atmospheric CO₂ concentration growth rate at Mauna Loa, Hawaii (MLO). The intent is to quantify the effect of El Niño and La Niña activity on the previously reported decreasing CO₂ sink rate with the most recent estimates of global emissions, and to provide a simple method for monitoring evidence of such decreases on a yearly basis in the future.

One way to describe how fast the Earth system removes excess CO₂ from the atmosphere is the airborne fraction, defined as the year-to-year change in measured CO₂ concentrations divided by yearly anthropogenic emissions [8]. The AF is loosely described as that fraction of humanity's yearly CO₂ emissions that remains in the atmosphere. Nature, however, does not 'know' how much CO₂ is emitted by anthropogenic activities each year, only how much CO₂ resides in the atmosphere. So, while the AF is a useful metric if anthropogenic emissions do not change abruptly, it can be shown that if all anthropogenic CO₂ emissions were to suddenly be cut in half, excess CO₂ would continue to be removed at about the same rate as before the emissions reduction, but the AF would suddenly become negative, which is clearly unphysical.

An alternative metric is the CO₂ sink rate, which is the fraction of the excess of atmospheric CO₂ above some natural baseline removed each year [6]. That baseline has been assumed to be the pre-industrial level near 280 ppm, but here that baseline is a model free parameter which is optimized based upon the MLO CO₂ data. R14 provides considerable detail about the advantages of the CO₂ sink rate and its sensitivity to various assumptions. The intent here is to use the sink rate along with the latest MLO observations of CO₂ concentrations during 1959 – 2021 together with the latest yearly estimates of global anthropogenic CO₂ emissions to calibrate a simple CO₂ budget model of year-to-year CO₂ changes in order to examine the sink rate's dependence on El Niño and La Niña activity.

How El Niño and La Niña activity is accounted for is critical. R14 also made ENSO adjustments to the data, but provided no details. It will be shown that the model residuals without accounting for ENSO activity during 1959-2021 are highly correlated (R=0.82) with El Niño Southern Oscillation activity as quantified by yearly averages of the Multivariate ENSO Index [9,10]. The ENSO effect is removed from the record to determine if the declining CO₂ sink rate is related to changing ENSO activity.

Finally, the model is extended to 2050 and beyond with the most recent Energy Information Administration estimates of future global CO₂ emissions to compare to various emissions scenarios used by Earth System Models (ESMs) to project future climate change [11].

1.1 The CO₂ Budget Model

Three-dimensional global carbon cycle models are very detailed, with complex representations of individual biological and geochemical processes on land and in the ocean [1,2]. Of course, such detail is necessary to understand which physical and biological processes on land and in the ocean are responding to increasing levels of atmospheric CO₂. Despite their complexity, the models still suffer from a lack of quantitative in situ measurements to better quantify the many sinks of excess atmospheric CO₂ [2].

Here, instead of complex individual carbon cycle processes, only the net response of the global carbon budget to increasing atmospheric CO₂ concentrations is addressed with a simple time-dependent CO₂ budget model. Roughly following Friedlingstein et al. and others, the yearly growth rate in atmospheric CO₂ (G_{atm}) is [1].

$$G_{atm} = dCO_2/dt = E_{FOS}(t) - S(t) + \beta MEI(t) \quad (1)$$

where the anthropogenic energy-related emissions source from fossil fuels EFOS comes from Boden et al. up to 2020, then from the Energy Information Administration estimates of yearly fractional changes in CO₂ emissions from 2021 to 2050 starting with the Boden value in 2020 [12,13].

The net land + ocean sink S of excess atmospheric CO₂ is

$$S(t) = k_s(CO_2(t) - CO_{2eq}), \quad (2)$$

where the yearly CO₂ sink rate (k_s) and the equilibrium value the CO₂ is relaxing to (CO_{2eq}) are both adjustable model parameters to optimize the model fit to Mauna Loa data.

The effect of El Niño and La Niña is represented with a constant of proportionality β in Eq. 1 and the monthly MEI values averaged from May (previous year) through April in the current year, after removing a +0.33 bias in the original MEI data (1950-2018) compared to the MEIv2 data (1979-2021) during their period of mutual overlap. As will be shown, May through April are the months which have the highest correlation ($r=0.83$) between MLO CO₂ changes and yearly average MEI values.

The model is initialized in 1750 at the CO_{2eq} value, and the three adjustable parameters of the model (CO_{2eq} , β , and k_s) are optimized to maximize the fit between model and observations during 1959-2021. The fit is evaluated with the correlation coefficient between the modeled and MLO observed CO₂ time series, and by minimizing the difference in 5-year average CO₂ concentration change between the beginning and the end of the modeled time series.

1.2. Model Fit to Mauna Loa Data

A critical test of the model is the validity of assumption represented by Eq. 2, that excess atmospheric CO₂ is removed at a rate proportional to how high the atmospheric CO₂ level goes above some inferred equilibrium CO₂ value the system is relaxing to. The value of ks does not have to remain constant over time, and there is evidence it has been decreasing since 1959 [7]. The CO₂ budget model provides a simple test to see if the MLO data suggest such a change is occurring, and its dependence upon ENSO activity.

The data-inferred value of the equilibrium level of CO₂ (CO_{2eq}) does not have to be the same as the pre-industrial value of CO₂ (~280 ppm), although one would expect it to be close to that value. In the context of the model it is the atmospheric level of CO₂ the MLO data suggest the system has been relaxing to during 1959-2021.

The best model fit to MLO data during 1959-2021 occurs with the CO_{2eq} = 293.6 ppm, ks = 0.0202, and β = 0.457. The comparison between model and MLO observations is shown in Fig. 1.

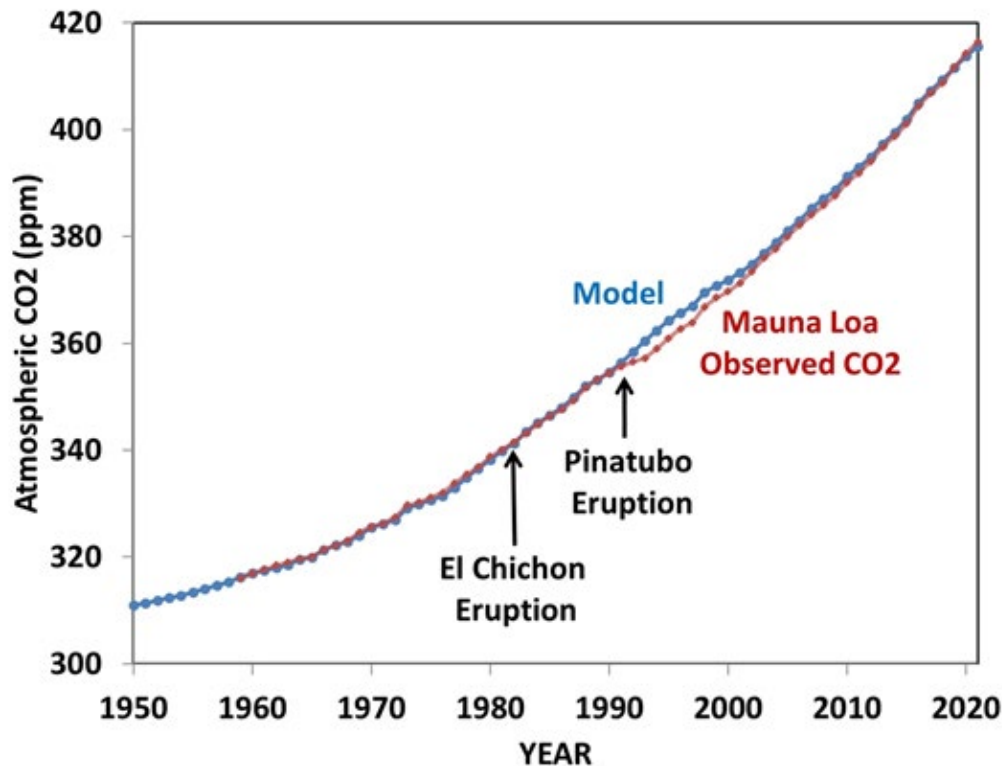


Figure 1: Model versus observed CO₂ at Mauna Loa, HI during 1959-2021, with ENSO effects included.

While an excellent fit between model and observations is obtained when CO_{2eq} = 293.6 ppm, use of the pre-industrial value of 280 ppm cannot be made to result in a model fit to the observations, even after adjusting ks. For example, if the model is forced to fit the MLO data in the last year of record (2021), its CO₂ concentration in 1959 is much (11 ppm) too low. While the reason for this is not clear, in the context of the model assumptions it indicates that the carbon cycle during 1959-2021 is relaxing to a higher equilibrium value of atmospheric CO₂ than the pre-industrial value of 280 ppm.

Note that the largest deviations of the model from observations are after the 1991 eruption of Mt. Pinatubo. During the post-Pinatubo period, increased diffuse solar radiation is believed to have caused increased photosynthesis due to deeper penetration of sunlight into

vegetation canopies (Gu et al., 2003), resulting in a faster terrestrial uptake of CO₂ [14].

Note that β=0.457 means that for a +/-1 unit change in MEI, there is a +/- 0.457 ppm yr⁻¹ change in atmospheric CO₂. Since R14 also accounted for ENSO activity, it is important to describe how β=0.457 was obtained. The MEI term β was optimized by running the model with β=0 and correlating the model-vs-observations residuals with one-year average MEI data, ending in various calendar months. This resulted in a 0.825 correlation coefficient between model residuals and MEI during non-volcanic years (Figure. 2) using the April through March averaging period.

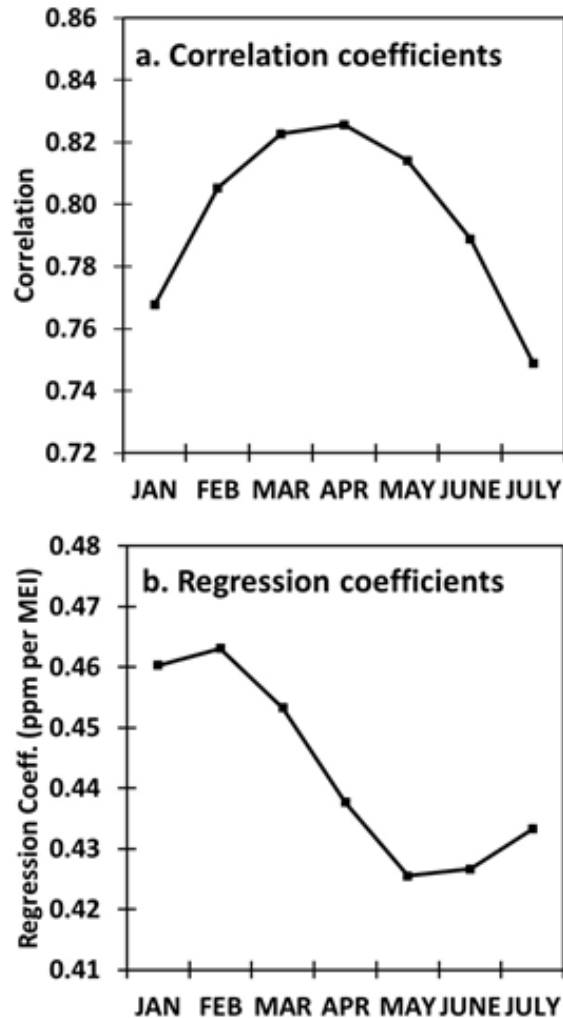


Figure 2: Correlation (a) and regression (b) coefficients between yearly average MEI ending in the indicated calendar months and the CO₂ model residuals when the model was run without an ENSO term included. Calculations exclude the volcanic years of 1983, 1991, 1992, and 1993 (see Figure. 3 for the large dCO₂/dt excursions in those years).

The importance of accounting for ENSO effects in the model is shown in Figure. 3a, where the CO₂ sink rate is seen to decrease without accounting for ENSO, but becomes essentially constant at 2.02% when the ENSO term is included. This is in contrast to the R14 results where a substantial downward trend in ks remained even after accounting for ENSO effects. Removal of the volcanic

years 1983, 1991, 1992, and 1993 in Fig. 3a had virtually no impact on the trends, likely due to their placement near the middle of the time series. Further study is necessary to determine whether it is the treatment of ENSO, the longer time period addressed here, or the updated estimates of global CO₂ emissions that is responsible for the difference between these results and those of R14.

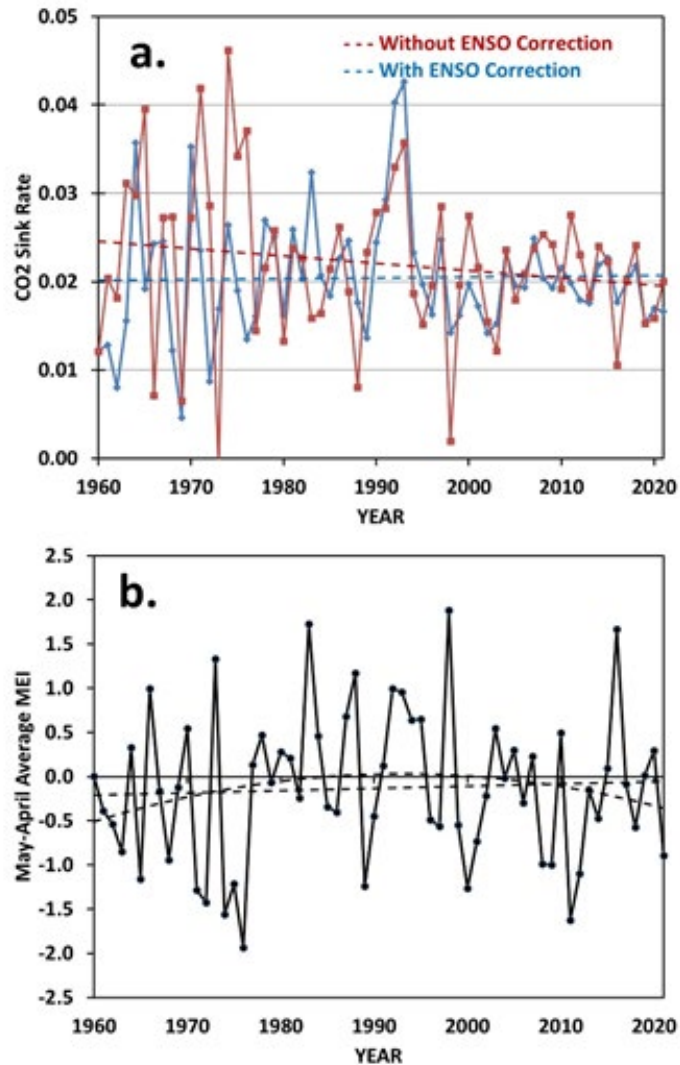


Figure 3: (a) CO₂ sink rate by year, with and without ENSO (El Niño and La Niña) effects being removed, and (b) yearly-average (April through March) MEI data used in the model to remove ENSO effects

Without correcting for ENSO activity k_s decreases at a relative rate of about -0.33% per year, which is somewhat weaker than the -0.54% per year value reported by Bennedsen et al. for the 1959-2016 period using a sophisticated statistical analysis [12].

1.3. CO₂ Concentration Projections to 2050 and 2100

Assuming the CO₂ sink rate remains constant and using the most

recent EIA estimates of yearly growth in global CO₂ emissions from 2011 to 2050 (Nalley and LaRose, 2021) for their three assumed cases -- reference, high economic growth, and low economic growth -- the model produces the CO₂ concentrations shown in Figure. 4. Of course, if the sink rate decreases substantially in the future, the projected concentrations will rise more rapidly.

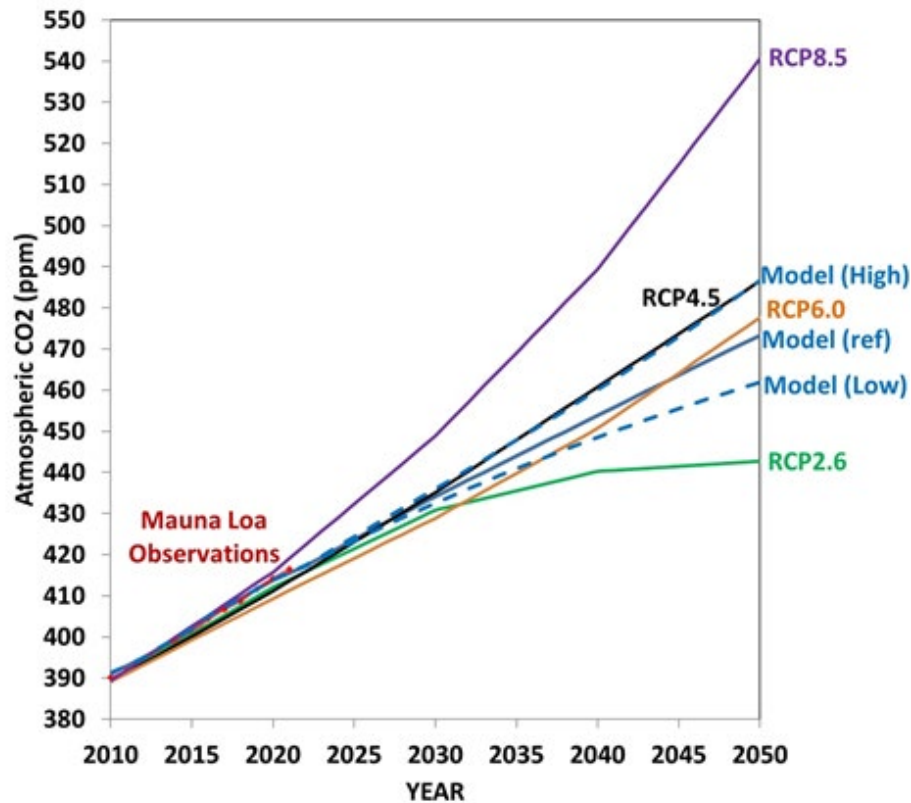


Figure 4: Atmospheric CO₂ concentrations during 2010-2050 from MLO observations (red), the CO₂ model using a constant CO₂ sink rate with three EIA assumptions regarding future global economic activity (blue), compared to the four IPCC RCP scenarios, RCP8.5, 6.0, 4.5, and 2.6.

The model produces an atmospheric CO₂ concentration of 473 ppm in 2050 for the EIA reference case using the model-optimized CO₂ sink rate of 0.0202. While one might argue that global carbon cycle changes could still cause ks to significantly decrease before 2050 (despite a lack of evidence from Figure. 2a, after correction for El Niño and La Niña), it should be remembered that for the period starting in 1959, 2021 is already 68% of the way to 2050. Of course, the model presented here would allow experimentation using various assumptions regarding a decreasing CO₂ sink rate.

The EIA estimates of yearly CO₂ emissions increases for their reference case remain nearly constant at +0.67% per year from 2030 through 2050, primarily due to emissions growth in non-OECD countries [13]. Emissions beyond 2050 are, of course, highly uncertain. For the sake of illustration, if we conservatively assume the same yearly emissions increases projected by the EIA during 2030-2050 will continue through the end of the century (a “business as usual” scenario), we obtain the model CO₂ estimates shown in Figure. 5.

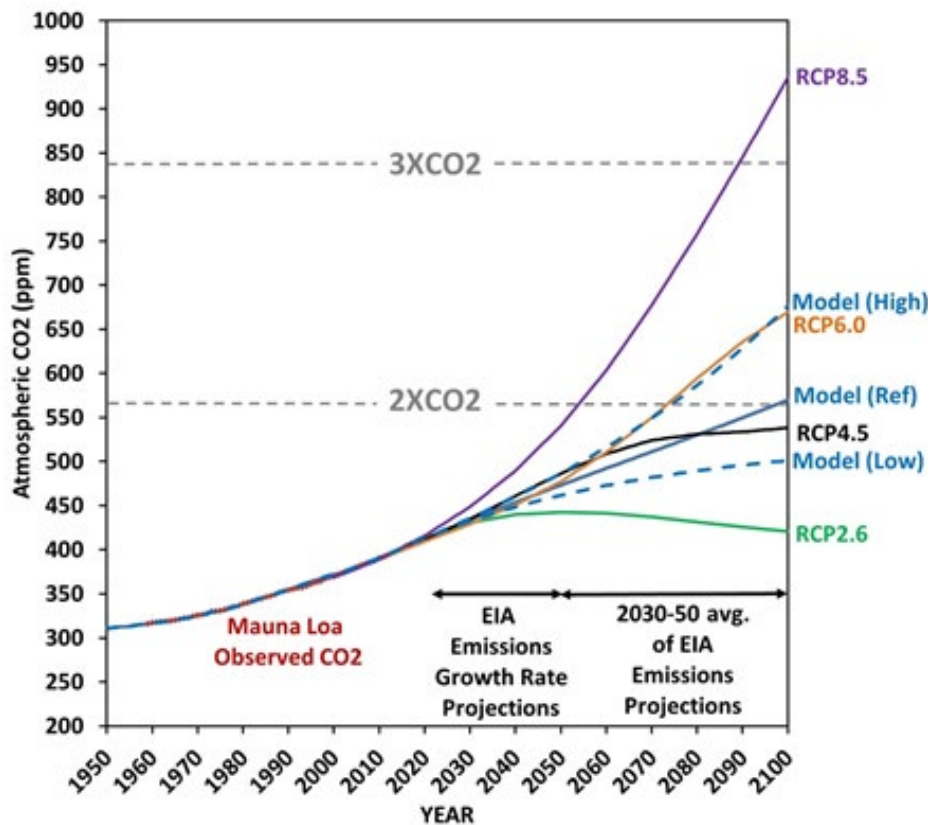


Figure 5: As in Figure. 4, but with the EIA-estimated emissions increases during 2030-2050 (0.67% per year) extended to 2100.

The reference case model CO₂ concentration in 2100 is 570 ppm, which is approximately double the putative pre-industrial value of 280 ppm. Significantly, it falls between the RCP4.5 and RCP6.0 emissions scenarios, and well below the RCP8.5 scenario which leads to the most severe climate change projections. Again, these scenarios depend greatly on assumed future anthropogenic emissions, as well as the assumption of a non-declining CO₂ sink rate.

On the climate side of the global change issue, the significance of lower future levels of atmospheric CO₂ in response to a non-declining CO₂ sink rate would be weaker climate change impacts. But on the global carbon cycle side, it would mean greater rates of carbon uptake by the land and ocean [15].

2. Discussion and Conclusions

The processes which control the rate of removal of excess CO₂ from the atmosphere are numerous and complex, involving physical and biological processes over land and in the ocean. While modeling that complexity is necessary to understand how the Earth system will respond to continued anthropogenic CO₂ emissions, there is also value in simple quantitative evaluations of how the Earth system has already responded to more atmospheric CO₂ employing simple but testable assumptions applied to accurate measurements of atmospheric CO₂ concentrations.

Using a basic time-dependent global-average CO₂ budget model

forced with yearly estimates of global anthropogenic CO₂ emissions, it is demonstrated that during 1959 to 2021, excess CO₂ is being removed from the atmosphere at a nearly constant rate of 2.0% per year of the difference between the atmospheric CO₂ concentration and an observations-inferred equilibrium level of 293.6 ppm, after accounting for ENSO (El Niño and La Niña) activity. This contrasts with the results of R14 where a substantial downward trend in ks was observed, even after accounting for ENSO. As shown in Figs. 4 and 5, the impact of a non-declining sink rate would be to keep future atmospheric CO₂ concentrations well below the most extreme scenario RCP8.5 based upon three recent EIA global emissions scenarios, with values during 2050-2100 more in line with the RCP4.5 to RCP6.0 scenarios. This would then lead to somewhat weaker climate change impacts in response to anthropogenic greenhouse gas emissions. It is not known to what extent the ENSO removal methodology, longer time period addressed here, updated global emissions estimates, or some other factor is responsible for this difference in CO₂ sink rate results compared to R14.

The largest departure of the model from observations is after the 1991 eruption of Mt. Pinatubo, when the CO₂ sink rate approximately doubled for two years. This has been previously attributed to increased photosynthesis due to more diffuse solar radiation penetrating vegetation canopies.

After the model is optimized to fit the Mauna Loa observations, it was run with EIA projections of global CO₂ emissions through 2050, as well as extrapolation of the 2030-2050 yearly increases out to 2100. The resulting CO₂ concentrations by 2050 and 2100 are between the IPCC RCP4.5 and RCP6.0 scenarios, and well below the RCP8.5 (extreme emissions case) scenario.

The fact that the Mauna Loa CO₂ data suggest an atmospheric equilibrium level of ~294 ppm, rather than the pre-industrial value of ~280 ppm, might indicate the Earth system carbon cycle has adjusted to a new equilibrium level during the Mauna Loa period of monitoring. This conclusion is speculative. If so, it could be that a time-dependent value for the equilibrium level would be more appropriate, but the Mauna Loa record is not sufficiently long to determine if this is the case. As mentioned above, this is a limitation of the empirical approach taken here to explain the Mauna Loa CO₂ record, without the underlying physical and biological processes contained in detailed global carbon cycle models.

The model can be used for conceptually simple, yet quantitatively meaningful, comparisons to the output of more complex models. The fact that such a good fit of the model to the observations is achieved with a nearly constant yearly CO₂ sink rate of 2.0% is rather remarkable. As additional years of Mauna Loa data become available, the testing of the simple model with each new year of data would allow determination if the rate of removal of excess CO₂ from the atmosphere is continuing at the previous rate, or if more complex and non-linear processes are occurring which might lead to higher CO₂ levels than those produced here. Also, improved estimates of anthropogenic CO₂ emissions, including changing land use patterns, should help improve the model agreement with observations, leading to more confident identification of future decreases in the CO₂ sink rate.

Acknowledgments

This research was funded through U.S. Department of Energy contract DE-SC0019296 and the Alabama Office of the State Climatologist. The author declares no financial or affiliation conflicts of interest.

Data Availability Statement

The CO₂ budget model, including the input datasets used, is in a single Excel file publicly available at [https://github.com/royw-spencer/CO₂-model/](https://github.com/royw-spencer/CO2-model/).

References

1. Friedlingstein, P. and et al. (2022). Global carbon budget 2021. *Earth System Science Data*, 14, 1917-2005.
2. Canadell, J. G., Monteiro, P. M., Costa, M. H., Da Cunha, L. C., Cox, P. M., Eliseev, A. V., ... & Lebehent, A. D. (2021). Global carbon and other biogeochemical cycles and feedbacks.
3. Gloor, M., Sarmiento, J., Gruber, N. (2010). What can be learned about carbon cycle climate feedbacks from the CO₂

- airborne fraction? *Atmospheric Chemistry and Physics*, 10.
4. Frölicher, T. L., Joos, F., Raible, C. C., & Sarmiento, J. L. (2013). Atmospheric CO₂ response to volcanic eruptions: The role of ENSO, season, and variability. *Global Biogeochemical Cycles*, 27(1), 239-251.
5. Raupach, M. R. (2013). The exponential eigenmodes of the carbon-climate system, and their implications for ratios of responses to forcings. *Earth System Dynamics*, 4(1), 31-49.
6. Raupach, M. R., Gloor, M., Sarmiento, J. L., Canadell, J. G., Frölicher, T. L., Gasser, T., ... & Trudinger, C. M. (2014). The declining uptake rate of atmospheric CO₂ by land and ocean sinks. *Biogeosciences*, 11(13), 3453-3475.
7. Bennedsen, M., Hillebrand, E., & Koopman, S. J. (2019). Trend analysis of the airborne fraction and sink rate of anthropogenically released CO₂. *Biogeosciences*, 16(18), 3651-3663.
8. Van Vuuren, D. P., Edmonds, J., Kainuma, M., Riahi, K., Thomson, A., Hibbard, K., ... & Rose, S. K. (2011). The representative concentration pathways: an overview. *Climatic change*, 109, 5-31.
9. Canadell, J. G., Le Quéré, C., Raupach, M. R., Field, C. B., Buitenhuis, E. T., Ciais, P., ... & Marland, G. (2007). Contributions to accelerating atmospheric CO₂ growth from economic activity, carbon intensity, and efficiency of natural sinks. *Proceedings of the national academy of sciences*, 104(47), 18866-18870.
10. Rasmusson, E. M., & Carpenter, T. H. (1982). Variations in tropical sea surface temperature and surface wind fields associated with the Southern Oscillation/El Niño. *Monthly Weather Review*, 110(5), 354-384.
11. Wolter, K. (1993). Monitoring ENSO in COADS with a seasonally adjusted principal component index. In *Proc. of the 17th Climate Diagnostics Workshop*, 1993.
12. Boden, T., Marland, G., Andres, R. J. (1999). Global, Regional, and National Fossil-Fuel CO₂ Emissions (1751 - 2014) (V. 2017). Carbon Dioxide Information Analysis Center (CDIAC), Oak Ridge National Laboratory (ORNL), Oak Ridge, TN. [Dataset]. ESS-DIVE repository.
13. Nalley, S., LaRose, A. (2021). International Energy Outlook 2021. U.S. Energy Information Administration, available at [Dataset] Outlook cases of world carbon dioxide emissions by region (Table A10)
14. Gu, L., Baldocchi, D. D., Wofsy, S. C., Munger, J. W., Michalsky, J. J., Urbanski, S. P., & Boden, T. A. (2003). Response of a deciduous forest to the Mount Pinatubo eruption: Enhanced photosynthesis. *Science*, 299(5615), 2035-2038.
15. van Marle, M. J., van Wees, D., Houghton, R. A., Field, R. D., Verbesselt, J., & van der Werf, G. R. (2022). New land-use-change emissions indicate a declining CO₂ airborne fraction. *Nature*, 603(7901), 450-454.

Copyright: ©2023 Roy W Spencer. This is an open-access article distributed under the terms of the Creative Commons Attribution License, which permits unrestricted use, distribution, and reproduction in any medium, provided the original author and source are credited.